Webology (ISSN: 1735-188X)
Volume 19, Number 2, 2022

Identification Of Chromatographical Characteristics Of Complicated Biological Feeds

[1*]Mr. Ganesh Babu Loganathan , [2]Ms. Amani Tahsin Yasin

[1]Assistant Professor, Department of Mechatronics, Faculty of Engineering, Tishk International University-Erbil, Kurdistan Region, Iraq.

[2]Assistant Lecturer, Department of Pharmaceutical Basic Sciences, Faculty of Pharmacy, Tishk International University-Erbil, Kurdistan Region, Iraq.

Abstract

Model parameters must be exact in order to employ mechanistic models in chromatography. Cleared cell harvest is particularly difficult feedstock for mechanistic models to simulate. A lack of specimen complex and time to establish all of the desirable criteria is also a big hindrance in the way. Therefore, the research's purpose was to build a process that initiates with complicated feedstock including monoclonal antibodies and uses an automated liquid handling system. It was put to the test by comparing separate data sets with estimates produced by the mechanical typical employing all parameters determined in this work. The method was backed up by a near-perfect match between predicted and actual results. The 200 L bed volume of Robo Columns may therefore be effectively used to regulate isotherm parameters for bigger scale column predictions. Mechanistic chromatographic modelling of complex biological feedstocks can benefit greatly from this approach since it provides a new way of finding crucial model input parameters.

Keywords : Chromatography, Biological feeds, Robo columbs, feedstocks, Isocratic

Introduction

In today's world, detailed models for predicting chromatographic behaviour are accessible. To simulate chromatograms with little uncertainty correct model input parameters are required. Some of these, such as packing and mass transport parameters are quite simple to determine[1]. Others, such as adsorption parameters, are more difficult to deal with, especially when dealing with complex biological feedstocks. The inverse technique is a widely used method for determining such adsorption parameters[2], [3]. It doesn't matter if the found residual is minimal, applying a strategy to minimise the discrepancy among investigational chromatograms and mechanistic prototype can result in erroneous values[24-31]. Furthermore, unique parameters are difficult to distinguish amongst contaminants eluting under nearly comparable conditions[4]–[6]. It is also possible to conduct high-throughput batch uptake tests as an alternative strategy [32-37]. For low protein concentrations and big macromolecules, the constraints achieved may not be exact those identified

in chromatography columns[7]. Column isocratic and linear gradient testing may be advantageous in some cases [38-45]. Fractionation technologies have been utilised in the past to apply methods that necessitate column trials to difficult feedstocks[8]–[11]. It then went on to use pH gradient prefractionation, gradient experiments and using Robo Columns having bed volume of only 210 litres, size exclusion was used to obtain isotherm parameters, in a 3D liquid chromatography technique to further minimise sample complexity[12].

One of the main goals of this paper is to build a more efficient and time-consuming high-throughput technique for determining input parameters of complicated biological feedstocks[13]. Using [14]'s method, robotic handling systems can be parallelized also saved time by using this article [46-55]. The method can also be used to get adsorption characteristics for the complete series of protein concentrations observed in manufacturing developments[15], [16]. In high-throughput batch-uptake studies, the resin of interest's maximum binding capacity is measured from fractions of the first dimension [71-84]. Protein aggregation behaviour is typically described using the second virial coefficient [56-69]. Furthermore, it was once used in the development of a chromatography isotherm[17].

Mechanistic chromatography model

Using the mass balance for phase, the symmetry transport diffusive model may define what happens inside a chromatography column as follows:

$$\frac{\partial c_i}{\partial t} + \frac{1-\varepsilon_b}{\varepsilon_b}\frac{\partial q_i}{\partial t} = -v\frac{\partial c_i}{\partial x} + D_{L,i}\frac{\partial^2 c_i}{\partial x^2} \qquad (1)$$

Particle concentration distributions are not considered in this model. Because of its simplicity and generally high degree of accuracy, this model is commonly employed. Liquid mass transfer was based on linear driving force to replicate changes in q_i, the concentration of protein I over time in stationary phase experiments (Equation 2).

$$\frac{\partial q_i}{\partial t} = k_{ov,i}\left(c_i - c_{p,i}^{*}\right) \qquad (2)$$

Mass transfer coefficient ($k_{ov,i}$) calculating the concentration in particle pores can be done using an appropriate adsorption isotherm. The following mixed mode isotherm, which is applicable to mixed mode chromatography, ion-exchange chromatography, and hydrophobic interaction in a nonlinear concentration range, is a good example of Mollerup's thermodynamic framework.

$$\frac{q_{p,i}}{c_{p,i}} = A_i\left(1 - \sum_{j=1}^{m}\frac{q_{p,j}}{q_{p,j}^{max}}\right)^{v_i+n_i} \qquad (3)$$

The fraction of free ligands is shown in the term $1 - \sum_{j=1}^{m}\frac{q_{p,j}}{q_{p,j}^{max}}$, where q_p^{max} signifies the highest binding capacity; m is the number of proteins and j is meant for the protein species. If A_i is a partition coefficient, we can use the following formula to find the starting slope of our isotherm:

$$A_i = K_{eq,i}\Lambda^{(v_i+n_i)}(z_s c_s)^{-v_i} c_v^{-n_i}\gamma_i \qquad (4)$$

$$A_i = K_{eq,i}\Lambda^{(v_i+n_i)}(z_s c_s)^{-v_i} c_v^{-n_i} \qquad (5)$$

The size exclusion and thermodynamic properties of a protein, as represented by the partition coefficient, affect its retention. As a result, the following equation can be used to relate retention factor to partition coefficient:

$$k_i = \frac{(1-\varepsilon_b)\varepsilon_p K_{D,i}}{\varepsilon_b}(1 + A_i) \qquad (7)$$

When the resin's accessibility to each protein I is indicated by the distribution coefficient, $K_{D,i}$. It is important to examine the influence of protein-protein interactions at higher protein concentrations. One can deduce that interactions between proteins of a single protein species are the most important in a complex mixture if that protein species is the dominant one. As a result, the following is a rough estimate of the molar activity coefficient:

$$\ln \gamma_i = 2B_{ii}c_{p,i} + \cdots \qquad (8)$$

To calculate the second osmotic virial coefficient (B_{ii}), or (B_{22}) use the following formula, which accounts for departures from ideal behaviour caused by interactions between two proteins of the same species. More than two molecules were considered to have insignificant interactions. Chloride has a modest salting-out impact, the activity coefficient for the most common protein species was simply defined as:

$$\gamma_i = e^{2B_{22}c_{p,i}} \qquad (9)$$

Material & methods

Gradient chromate focussing prefractionation

A 1.3mg/mL monoclonal immunoglobulin G (IgG1)-containing cleared CHO cell culture supernatant was used in this study as the complex sample. Capillary isoelectric focusing was used to calculate the pl of IgG1, which came out to 8.6. Before use, the samples were rebuffered using disposable PD-10 columns according to the manufacturer's instructions. The samples were separated using linear pH-gradient chromatography on a Mono Q 4.6/100 strong anion exchange column or a Mono S 4.6/100 strong cation exchange column.

Column characterization

The columns used are 210 liter Robo Columns packaged through two distinct resins, as shown in Table 1. Dextrans retention volumes ranging from 180-6300000 Da were measured using a 1100 series refractive index detector. In order to figure out the K-D distribution coefficient, we did the following:

$$K_D = \frac{\frac{\mu_1}{V_{col}} - \varepsilon_b}{1-\varepsilon_b} \qquad (10)$$

the mean retention volume or initial instant of the peak, which is generally recorded without a column connected and the dead volume in the column itself, has been corrected to provide a value of 1. Robo Columns have a smaller column volume(V_{col}) to column volume ratio, which makes the

column dead volume critical. It was discovered to be 30.L in previous investigations. For packed chromatographic columns, the bed porosity,-b. is usually between 0.3 and 0.4.

Following equations (10 and 11) were used to fit MATLAB's function / sq curve fit to K_D data to obtain the intraparticle porosity $\varepsilon_{p,n}$, and pore radii, $r_{pore\ ,n}$,:

$$K_{D,n} = \left(1 - \frac{r_h}{r_{pore,n}}\right)^2 \qquad (11)$$

A resin with POROS 50 HS has two distinct pore types (n). Dextran hydrodynamic radii were computed using an empirical correlation given in [24]($r_h = 0.0271M^{0.498}$).. There are two sorts of pore types in the resin, so the total intraparticle porosity was computed as the sum of the macropores $\varepsilon_p = \varepsilon_{p,1} + \varepsilon_{p,2}$ and the micropores: n=1 signifies the macropores and n=2 signifies the micropores. K_D of the two pores is defined as follows

$$K_D = \varepsilon_{p,1}K_{D,1} + \varepsilon_{p,2}K_{D,2} \qquad (12)$$

Isocratic chromatography

These systems do not contain dual-piston pumps or inline detectors. Single piston pumps are replaced by 96 well plates on a motorised shuttle that collect fractions at the column's exit and do offline analysis. The experimental design must be altered to accommodate these mechanical simplifications in order to get data that is equivalent to that obtained from experiments on more typical systems. Before each chromatographic experiment involving stock solutions, the liquid management system diverse an adequate volume of buffer for all column equilibration and elution. [18] was used to make two stock solutions, one with a low salt concentration and the other with a high salt concentration. A total of eight dissimilar salt concentrations in required ranges could be achieved by adjusting the mixing ratios. The resin and buffer specifications are shown in Table 1.

Table 1. Specifications for the resin and its buffer

Type of Resin	Type	Dp	pH	Type of Buffer	Buffer	Type of Salt	Range of Salt
Poros 50HS	Strong CEX	50	4.6	Acetic acid	30	NaOH	0-550
Capto MMC	MMC	85	6.80	MOPS	30	NaOH	0-400

Starting to injection 5 CV of elution buffer were used to balance every column. A 20-liter injection was administered to each column. A flow rate of 0.15 ml/min was used to elute the samples, which contained 15 CV of elution buffer per column. Through the isocratic elution, 22 samples were obtained from each column. An UV-star plate with a capacity of 75 litres collected the first 12 sections. Six more fractions with a goal volume of 150 µl were collected in a full area UV Star plate, followed by four more with a goal volume of 300µl. For this experiment, it was important to have a modest total number of fractions while still achieving high resolution at outset of

experimentation, hence the staggered fractionation method was employed[19], [20]. First 600 µl was collecting as two fractions, each with a 300 µl objective volume, and then the columns were washed using 5 CV of washing buffer.

We counted the number of data points in each chromatogram whose absorbance, measured at 230 nm, was more than the sum of its two neighbouring fractions to determine the number of peaks in that chromatogram. For this reason, only the four largest points on each chromatogram that satisfied these criteria were selected for further study[21]. When fitting a least squares peak model to the reconstructed chromatogram using this algorithm's height and location of local maxima, these were used as the first predictions.

The fitting function was derived using a one-dimensional adaptation of the model for multiple overlaid exponentially modified Gaussian peaks[22]. Instead than minimising the squares between the observed data point and the peak model's curve, the squares between this average and the measurement were minimised by averaging the model curve for each fraction interval.

Parameter fitting

Calculations of retention factors were based on the results of peak moments defined as k_i:

$$k_i = \frac{\mu_{1,i} - V_0}{V_0} \qquad (13)$$

The column's void volume V_{col} is denoted by the number V_0. In order to derive important isotherm parameters from experimentally measured peak moments, equations 5 and 6 can be used simultaneously. HIC (n) stoichiometry's coefficient can be set to zero when POROS 50HS is used. The adsorption isotherm of Capto MMC, a mixed-mode resin, was well described utilising only the ion exchange portion of the isotherm.

Batch uptake experiments.

The maximum capacity of the fractions containing IgG1 was also determined through additional research. Batch uptake tests in 96-well filter plates were used to achieve this. Packing density of Resiquot is lower than that of a packed column, therefore even while the volume dispensed is exact, fewer particles may be present than in a packed column. For POROS 50 HS, the provider recommended a factor of 1.06, which was applied in this investigation. For Capto MMC, there was no packing factor.

[23] provided a method for determining the liquid hold-up volume, or the amount of liquid remaining in the resin after centrifugation. Before use, 300 litres of the suitable buffer were used to acclimate the resin plaques. After 5 minutes of incubation at 1300 rpm, they were centrifuged at 4000g. A second round of equilibration was performed. Table 1 displays the buffer solutions that are relevant. Self-adhesive foil was used to keep them from evaporating. Additional batch absorption studies were carried out with a protein A pure sample of the product in order to verify its full potential.

Self-interaction chromatography

The concentration of IgG1 in the cleared cell harvest is significantly higher than that of any other protein. As a result, it was expected that just IgG1's motion coefficient and thus its second osmotic virial coefficient B_{22}, needed to be identified. By using pre-packaged HiTrap activated HP columns B_{22} was calculated on a Avant 25 chromatography system. The pH 8.5 coupling buffer contained 0.2 M $NaHCO_3$ and 0.5 M NaCl. A Protein A column was used to purify Synthon's IgG1 sample. Amicon Ultra 4 Centrifugal filters were used to replace the coupling buffer after centrifugation at 4000xg for 15 minutes[24]. All the samples had to be double-dissolved in the coupling buffer in order to avoid the formation of aggregates. The final solution contained 3 g/L IgG1. Recirculation over the column was carried out at a flow rate of 1 ml/min for four hours at a temperature of approximately 4°C. When the IgG1 eluent concentration was calculated at UV 280 nm, the amount of IgG1 adsorbed in column could be estimated for sure. Using the method described by[25], the surface coverage was calculated. Finally, the manufacturer's method deactivated any extra active groups, resulting in a surface coverage of 12.3 percent, which is within the recommended limit.

An additional HiTrap column was used to investigate the retention volume of IgG1 in the absence of protein-protein interactions, as described by [26]. It was created using the same deactivation procedure. This column is thought to be used solely as a size excluder. The following correlation was used to account for changes in integrity in the experiments conducted in the blocked column for each solution condition:

$$V_0 = aV_{0,b} + b \qquad (14)$$

Data on the retention of the immobilised column's immobilised acetone and dextrane are used to compute values for a and b. 2g/L blue dextran in 50mM Tris-HCl and 100m buffer at pH7.5 was added to the 50L acetone solution and the 1MNaCl was added for the blue dextran elution, which eluted at 1mL/min. . The values of a and b were found to be 0.25 and 0.32, respectively.

Both buffers and salt concentrations were tested on each column in duplicate to determine the retention volumes for IgG1. A flow rate of 0.5 mL/min was used to equilibrate the columns with 10CV of the appropriate buffer. Using a 1.5g/L protein concentration, the buffer was flushed with 5CV of the appropriate buffer and the protein injected into it. With 0.5M NaCl, the column rinsed three times with 3CV.

MATLAB's fit function with robust bisquare weights approach is used to fit a second order polynomial function to the determined B22 values. The following is the definition of the polynomial:

$$B_{22} = b_1 + b_2 pH + b_3 c_S + b_4 pHc_S + b_5 pH^2 + b_6 c_S^2 \qquad (15)$$

Modelling techniques

There is a complete list of correlations that can be used to identify important factors in Table 2.

Table 2. Correlations in mass transfer

S.No	Parameter	Correlations

1	Diffusivity in the free state	Young
2	Coefficient of mass transfer in films	Wil and Geankoplis
3	Tortuosity of the Pores	Suzuki and Smith
4	Diffusivity of Pores	Brenner and Gaydos
5	Coefficient of axial dispersion	Gunn
6	Radius of hydrodynamics	Stokes Einstein

Results & discussion

Prefractionation and reference chromatogram

Figure 2 shows the results of the prefractionation tests, together with the two-dimensional maps that accompanied them. The protein of interest IgG1 is represented by peak 2 of the anion exchange prefractionation. A high molecular weight (HMW) contaminant, Peak 5, appears to have comparable charge properties as Peaks 1, 3, 4, 6, and 7 among the most common contaminants. According to the protein of interest, peak 9-17 has a significant variation in pH, which indicates that these contaminants can be eliminated easily and will be considered non-critical impurities in the future[27]. As a result, only the prefractionation chromatogram-identified fractions of interest were examined in depth. IgG1 is ID 1 in the prefractionation cation exchange method. The gradient eluted considerably fewer contaminants in this case, suggesting that anion exchange is a superior separation strategy. Peak 2 was the only significant impurity found.

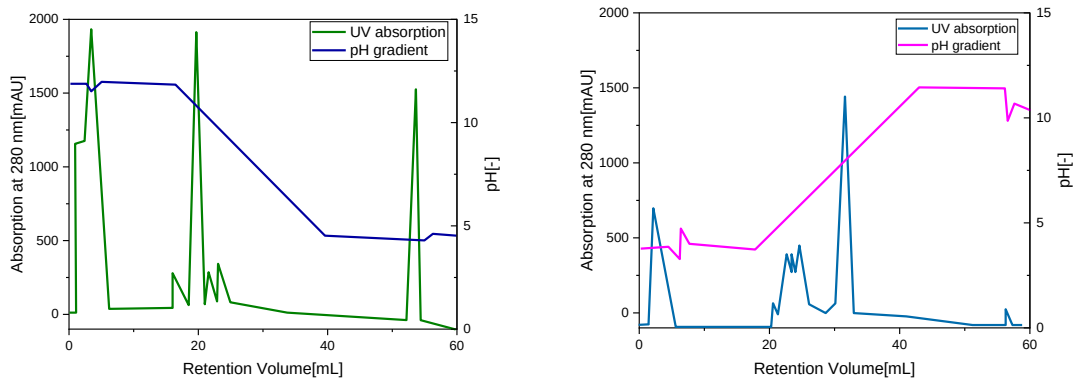

Figure 2: On the AEX and CEX columns, there is a prefractionation step. Interest fractions

High-throughput isocratic experiments

The regressed transmission coefficients were found to be 0.6400.001 mm/AU for the used buffer system NIR. All liquid buffer systems provided their density remains similar t that of pure water, absorb at approximately the same wavelength due to the buffer's water content. Full plate meniscus correction coefficients are 12.72 ± 0.35 µl/ln(Σ_{halo}) and half plate meniscus correction coefficients (C_{vm}) were determined to be 1.76± 0.30 µl/ln(Σ_{halo}) and 12.72±0.35 µl/ln(Σ_{halo}) respectively. Meniscus development was aided by a model protein, however these metrics were found to be unaffected by it. One can see how the logarithm of sum of measurements around well and volume which is not taken into account for truncated cone and so meniscus is depicted in Figure 3 a. Both

well geometries' linear connection justify using a basic linear model. In half-area plates, the meniscus volume is roughly 05 litres, while in full-area plates, it can exceed 35 litres, making up at least 10% of the total well capacity. The meniscus adjustment improves volume detection accuracy by more than 3% for full-area plates and 5% for half-area plates[28]. Figure 3 b shows the technique's accuracy across a wide range of volumes in all plate geometries. In half-area plates, precision seems to be mostly unaffected by volume, while in full-area plates, low volumes are definitely detrimental. In full-area plates, small quantities tend to be unevenly distributed around the well. As a result, for capacities ranging from 50 to 125 litres, half-area plates should be used and full-area plates should be utilised.

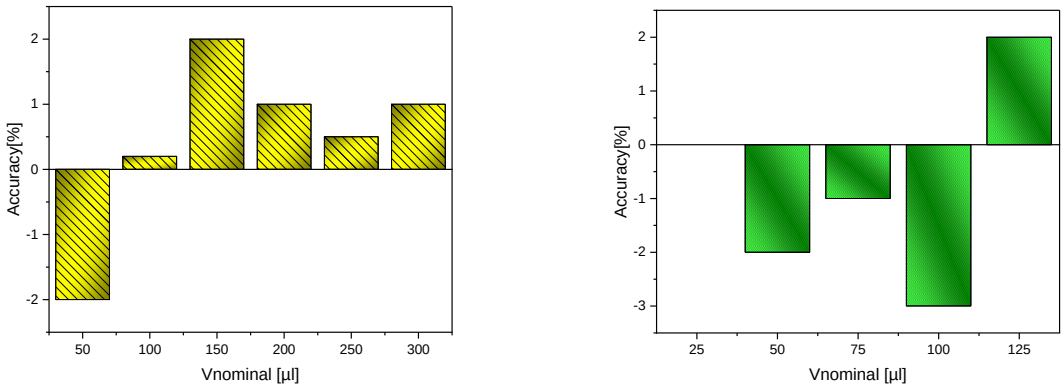

Figure 3: calibration of the meniscus-based volume detection method The method's average volume estimation accuracy in full- area plates (a) and half-area plates (b). Over the course of at least eight observations, the error bars represent a standard deviation of twice that value.

Resin and column characteristics

The Robo Columns were described using pulses of dextran standards. The following is a typical pattern for particles having bidisperse pore systems: Particle size has a direct effect on the BO curve, which begins to level out at roughly 10 nm, showing that macroporous access is now the primary factor in determining the curve's behaviour. In order to calculate porosity, the biggest dextran's retention volume cannot be used. All Robo Columns with the same resin, it was thought, had the same bed porosity (0.3 for POROS 50 HS and 0.35 for Capto MMC). Based on the Blake-Kozeny equation for linear flow, the bed porosity of the validation columns was identified to be 0.34 for POROS 50 HS and 0.36 for Capto MMC. With a hydrodynamic radius of 4.3 nm, IgG1 has difficulty accessing holes with a diameter of 8.2 nm. As a result of batch fluctuation, the micropore porosity is somewhat higher, but the other values measured here are in close agreement with those observed in POROS 50 HS.

Capto MMC-filled Robo Columns were subjected to the same procedure. As the pore distribution was considered monodisperse, a good match was proven to the data. A similar result for smaller hydrodynamic radii clearly shows that Capto MMC also has the same bidisperse distribution of pores for higher hydrodynamic diameters. In spite of having slightly larger pores and a higher porosity, POROS 50 HS behaves in a similar way. In addition, macropores have shrunk. It was easy

to predict the diffusion of pores by combining the diffusion of macropores with that of micropores and accounting for the relative porosities of each:

$$D_p = \varepsilon_{p,1} D_{p,1} + \varepsilon_{p,2} D_{p,2} \quad (16)$$

Table 3. POROS 50HS and Capto MMC resin properties are listed with their standard error.

	POROS 50 HS	**Capto MMC**
Macropore radius [nm]	372±76	165±23.56
Macropore porosity [-]	0.34±0.02	0.31±0.04
Micropore radius [nm]	11±4.16	12.46±0.76
Micropore porosity [-]	0.39±0.02	0.63±0.04
Total intraparticle porosity [-]	0.59±0.03	0.89±0.04

The isotherm calculation necessitates the use of the ligand density, which is a critical quantity in determining how well chemicals adhere to the resin (Equation 4 and 5). [29]–[31] provides the following information: Capto MMC was discovered to have an acid-base density of 0.128M per particle volume, whereas POROS 50 HS was found to have a ligand density of 0.27M.

Isocratic chromatography

Isocratic studies on Robo Columns holding the necessary resin at varied salt concentrations examined each percentage of interest. UV measurements were used to quantify the volume of the well from the fractions gathered in this study, which increased resolution and sensitivity. In ion exchange chromatography, the proteins (ID 3 and ID 4) elute earlier when the salt concentration rises, as is typical. Both proteins can be easily distinguished by using UHPLC measurements on the additional y-axis.

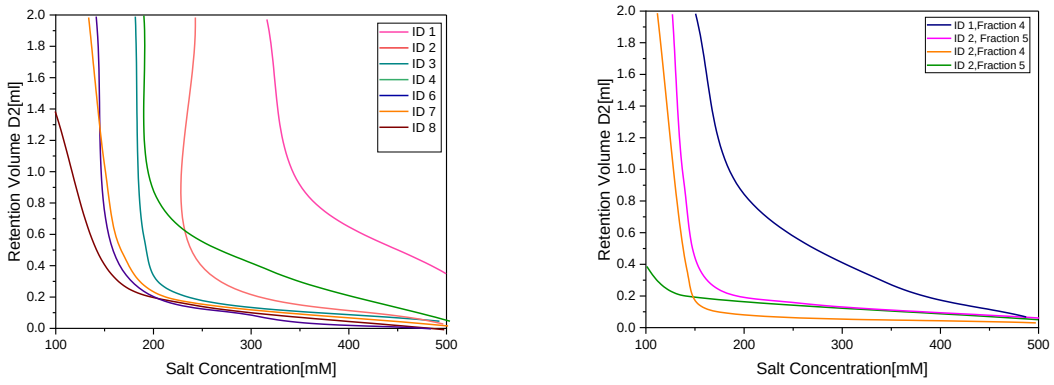

Figure 5: Retention volumes measured with POROS 50HS(a) and Capto MMC(b) Corresponding fitted curves for all essential proteins

The mean of the values fitted for every fraction is used to determine the final parameters for Capto MMC. There was no elution of protein ID 5 with salt concentrations utilised in the tests. We are therefore left without any information on the isotherm.

Batch-uptake experiments

Using maximal binding conditions, isotherms for antibodies purified with Protein A step and the prefractionated containing mostly the antibody were determined In order to see if even low amounts of contaminants had an impact on the maximum binding capacity, we tested both types of samples. All pollutants were assumed to enter the pore space that IgG1 was unable to use because of their lower size.

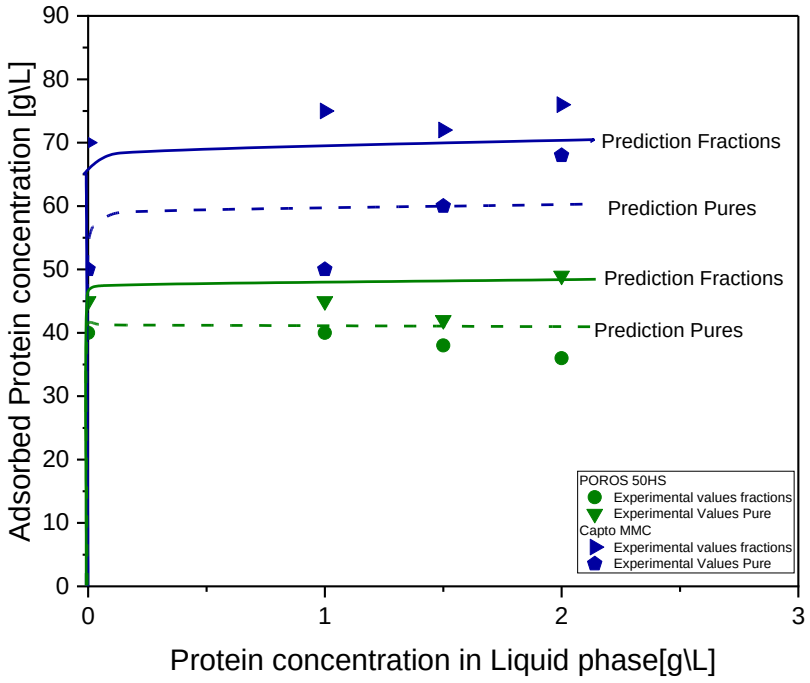

Figure 7: Maximum capacity for mAb on POROS 50 HS and Capto MMC are identified. Robo Column trials at the maximum capacity yielded the isotherm slope, which was used as a fitting parameter to generate the projected lines. Over 3 g/L values are not shown.

A slight difference in the buffer solution's ionic strength, which was not assessed, could explain the results of the Capto MMC antibody experiments. The ionic strength in every well should be measured right in future studies.

In general, there was a strong correlation between the predicted and experimental outcomes. In order to fit the polynomial, two extra experimental data points are discovered that is not comprised in original data set.

Table 4. The second order polynomial multiplied by 10-4 contains all of the constants.

	b_1	b_2	b_3	b_4	b_5	b_6
Acetate buffer	6.628	-2.491	1.346	-0.612	0.243	1.524
MOPS buffer	2.114	-0.813	-0.206	0.218	0.039	-0.903

Model validation

Finally, the mechanistic model was utilised to simulate the essential proteins using all of the determined parameters as model input parameters. Experiments with clarified cell collection were carried out at lab scale under identical settings to assess the model's correctness.

Dimerization or higher aggregation is what caused the tailing in the study by UHPLC. Apart from that, forecasts and experimental outcomes are quite closely aligned. One of two things can happen as a result of this. The most important contaminants were identified during prefractionation. In order for the purification process to be successful, it is imperative that the relevant chromatographic phase removes these dangerous pollutants. Robo Columns also make it possible to define isotherm parameters for low protein concentrations without the need for extra scale-up modifications. Packing characteristics and fluid dynamics are obviously affected. Protein-protein interactions can occur not just between two molecules, but also between multiple molecules, according to another theory about the molecules involved. In that case, it would be necessary to calculate higher virial coefficients. In our parameter estimation approach, no isotherm data for the dimer was provided, as the dimer did not form under the conditions required. Retention data for IgG1 was fit again, this time using a BO that was twice as large as the original one.

5. Conclusion

Use a high-speed workstation to estimate isotherm parameters for a cell harvest containing monoclonal antibodies, as detailed in this study. The pure cell harvest was initially separated in order to minimise the mixture and identify the most important proteins. Second, isocratic column tests using Robo Columns yielded isotherm parameters in the linear protein concentration range of the isotherm from the acquired fractions. In order to determine the resin's maximal capacity, batch uptake investigations were conducted. Fourth, the second osmotic virial coefficient for IgG1 was determined using self-interaction chromatography in order to define protein-protein interactions. After then, the mechanistic model was tested in a lab setting with all of the data that had been obtained throughout the course of the investigation. The predicted and simulated chromatograms were in good agreement with each other. To summarise: Robo Column data may be used to simulate larger scale columns, which is the study's most notable discovery. That supports our idea that focusing on the essential molecules is sufficient.

If one protein say IgG1 is in higher proportion than the others in a mixture like the one studied, then certain assumptions can be made. If this were not the case, it would be necessary to identify the maximum capabilities of other proteins. Having a higher concentration of proteins might alleviate this worry. Second virial coefficient assumption would be wrong as well.

A high-throughput workstation might be used to perform all tests (except prefractionation) in this study, which would boost automation and reduce sample consumption. Only the size-exclusion chromatography and self-interaction chromatography would need to be changed or improved, necessitating additional study.

For chromatographic mechanistic modelling, the proposed technique provides trustworthy parameters. With model-based process development, a product can be brought to market more quickly and at a lower cost.

References

1. V. Kumar, S. Leweke, E. von Lieres, and A. S. Rathore, "Mechanistic modeling of ion-exchange process chromatography of charge variants of monoclonal antibody products," J. Chromatogr. A, vol. 1426, pp. 140–153, 2015.
2. A. Osberghaus, S. Hepbildikler, S. Nath, M. Haindl, E. von Lieres, and J. Hubbuch, "Determination of parameters for the steric mass action model—A comparison between two approaches," J. Chromatogr. A, vol. 1233, pp. 54–65, 2012.
3. N. Marchetti, A. Cavazzini, L. Pasti, and F. Dondi, "Determination of adsorption isotherms by means of HPLC: adsorption mechanism elucidation and separation optimization," J. Sep. Sci., vol. 32, no. 5-6, pp. 727–741, 2009.
4. N. Borg, K. Westerberg, N. Andersson, E. von Lieres, and B. Nilsson, "Effects of uncertainties in experimental conditions on the estimation of adsorption model parameters in preparative chromatography," Comput. Chem. Eng., vol. 55, pp. 148–157, 2013.
5. K. M. Lacki and E. Brekkan, "High throughput screening techniques in protein purification," Methods Biochem Anal, vol. 54, pp. 489–506, 2011.
6. T. Bergander, K. Nilsson-Välimaa, K. Öberg, and K. M. Lacki, "High-throughput process development: determination of dynamic binding capacity using microtiter filter plates filled with chromatography resin," Biotechnol. Prog., vol. 24, no. 3, pp. 632–639, 2008.
7. B. K. Nfor et al., "Multi-dimensional fractionation and characterization of crude protein mixtures: toward establishment of a database of protein purification process development parameters," Biotechnol. Bioeng., vol. 109, no. 12, pp. 3070–3083, 2012.
8. A. T. Hanke et al., "3D-liquid chromatography as a complex mixture characterization tool for knowledge-based downstream process development," Biotechnol. Prog., vol. 32, no. 5, pp. 1283–1291, 2016.
9. A. Quigley and D. R. Williams, "The second virial coefficient as a predictor of protein aggregation propensity: a self-interaction chromatography study," Eur. J. Pharm. Biopharm., vol. 96, pp. 282–290, 2015.
10. T. Ahamed, M. Ottens, G. W. K. van Dedem, and L. A. M. van der Wielen, "Design of self-interaction chromatography as an analytical tool for predicting protein phase behavior," J. Chromatogr. A, vol. 1089, no. 1–2, pp. 111–124, 2005.
11. X. Xu and A. M. Lenhoff, "A predictive approach to correlating protein adsorption isotherms on ion-exchange media," J. Phys. Chem. B, vol. 112, no. 3, pp. 1028–1040, 2008.
12. J. M. Mollerup, "Applied thermodynamics: A new frontier for biotechnology," Fluid Phase Equilib., vol. 241, no. 1–2, pp. 205–215, 2006.

13. B. K. Nfor et al., “Model-based rational methodology for protein purification process synthesis,” Chem. Eng. Sci., vol. 89, pp. 185–195, 2013.
14. B. K. Nfor, M. Noverraz, S. Chilamkurthi, P. D. E. M. Verhaert, L. A. M. van der Wielen, and M. Ottens, “High-throughput isotherm determination and thermodynamic modeling of protein adsorption on mixed mode adsorbents,” J. Chromatogr. A, vol. 1217, no. 44, pp. 6829–6850, 2010.
15. J. M. Mollerup, T. B. Hansen, S. Kidal, and A. Staby, “Quality by design—thermodynamic modelling of chromatographic separation of proteins,” J. Chromatogr. A, vol. 1177, no. 2, pp. 200–206, 2008.
16. J. M. Mollerup, “The thermodynamic principles of ligand binding in chromatography and biology,” J. Biotechnol., vol. 132, no. 2, pp. 187–195, 2007.
17. T. L. Hill, “Thermodynamics for chemists and biologists,” 1968.
18. D. J. Winzor, L. E. Carrington, and S. E. Harding, “Analysis of thermodynamic non-ideality in terms of protein solvation,” Biophys. Chem., vol. 93, no. 2–3, pp. 231–240, 2001.
19. J. M. Prausnitz, R. N. Lichtenthaler, and E. G. De Azevedo, Molecular thermodynamics of fluid-phase equilibria. Pearson Education, 1998.
20. A. T. Hanke, P. D. E. M. Verhaert, L. A. M. van der Wielen, M. H. M. Eppink, E. J. A. X. van de Sandt, and M. Ottens, “Fourier transform assisted deconvolution of skewed peaks in complex multi-dimensional chromatograms,” J. Chromatogr. A, vol. 1394, pp. 54–61, 2015.
21. G. Carta and A. Jungbauer, Protein chromatography: process development and scale-up. John Wiley & Sons, 2020.
22. S. Zhang et al., “Structural and performance characteristics of representative anion exchange resins used for weak partitioning chromatography,” Biotechnol. Prog., vol. 33, no. 2, pp. 425–434, 2017.
23. Manoharan S, Sai Krishnan G, Babu L G, Vijay R and Singaravelu D L 2019 Synergistic effect of red mud-iron sulfide particles on faderecovery characteristics of non-asbestos organic brake friction composites Mater. Res. Express 6 105311.
24. Lokesh, P.; Kumari, T.S.; Gopi, R.; Loganathan, G.B. A study on mechanical properties of bamboo fiber reinforced polymer composite. Mater. Today Proc. 2020, 22, 897–903.
25. Sai Krishnan G, Jayakumari L S, Babu L G and Suresh G 2019 Investigation on the physical, mechanical and tribological properties of areca sheath fibers for brake pad applications Mater. Res. Express 6 085109.
26. Ganesh Babu L 2019 Influence of benzoyl chloride treatment on the tribological characteristics of Cyperus pangorei fibers based nonasbestos brake friction composites Mater. Res. Express 7 015303.
27. Devaraju, P. Sivasamy, Ganesh Babu Loganathan, “Mechanical properties of polymer composites with ZnO nano-particle”, Materials Today: Proceedings (2020), Volume 22, Part 3, Pages 531-534.
28. Ganesh Babu Loganathan, Dr. E.Mohan, R.Siva Kumar, “ Iot Based Water And Soil Quality Monitoring System”, International Journal of Mechanical Engineering and Technology (IJMET)(2019), Vol.10 Issue No.2, P.No. 537-541.
29. Krishnan GS et al (2020) Investigation of Caryota urens fibers on physical, chemical, mechanical and tribological properties for brake pad applications. Mater Res Exp 7:015310.

30. Ganesh Babu Loganathan, “Can Based Automated Vehicle Security System”, International Journal of Mechanical Engineering and Technology (IJMET)(2019), Vol.10 Issue No.07, P.No. 46-51.
31. C. Sivakandhan, Ganesh Babu Loganathan, Material characterization and unconventional machining on synthesized Niobium metal matrix Mater, Res. Exp. 7 (2020) 015018.
32. P Sivasamy, S Harikrishnan, L Ganesh Babu, S Imran Hussain, S Kalaiselvam, “Improved thermal characteristics of Ag nanoparticles dispersed myristic acid as composite for low temperature thermal energy storage” Materials Research Express, ISSN: 2053-1591, Volume-6, Issue-8, May 2019, P.No 085066.
33. Sundar Singh Sivam S P, Umasekar V G, Loganathan G B, Kumaran D and Rajendrakumar S 2019 Multi response optimization of setting process variables in face milling of ZE41 magnesium alloy using ranking algorithms and ANOVA International Journal of Vehicle Structures & Systems 5 47–56.
34. S.P.S.S. Sivam, G.B. Loganathan, K. Saravanan, V.G. Umasekar and S. Rajendrakumar. 2019. Numerical Evaluation and Influence of Product Quality and its Defects Measures on the Drawing of Stainless Steel Cross Member for Automobiles Int. J. Vehicle Structures & Systems, 11(1), 107-112. doi:10.4273/ijvss.11.1.19.
35. Sivam Sundarlingam Paramasivam, S., Loganathan, G., Kumaran, D., Saravanan, K. et al., "Function of Taguchi Grey Relation Analysis for Influencing the Process Parameter for Getting Better Product Quality and Minimize the Industrial Pollution by Coolants in Turning of Ti-6Al-4V Alloy," SAE Technical Paper 2019-28-0065, 2019, https://doi.org/10.4271/2019-28-0065.
36. Sivam SPSS, Loganathan GB, Umasekar VG, Suresh Kumar PS, Raja S (2019) Study on micro structural characteristics and mechanical behaviour of AISI1050 steel under various heat treatments. Int J Veh Struct Syst 11(1):15–20. https://doi.org/10.4273/ijvss.11.1.04.
37. Sivam S.P.S.S., Loganathan G.B., Saravanan K., Dinesh Guhan S., Banerjee A. (2021) Effects of Drilling Process Parameters Using ANOVA and Graphical Methods. In: Kumaresan G., Shanmugam N.S., Dhinakaran V. (eds) Advances in Materials Research. Spring
38. Mr.Vishwa Deepak, S.Nithish, D. V. B. M. B. L. M. (2021). Static Stress Analysis of an Addendum Modified Spur Gear Pair using FRP Material. Design Engineering, 3562-3573. Retrieved from http://thedesignengineering.com/index.php/DE/article/view/5301. ISSN 0011-9342,
39. Ganesh Babu Loganathan, K. I. M. G. (2021). CROWD CONTROL ROBOT FOR CONGESTION CONTROL. Design Engineering, 3377- 3391. Retrieved from http://thedesignengineering.com/index.php/DE/article/view/5286. ISSN 0011-9342,
40. Manikandan Ganesan, Ganesh Babu Loganathan, J.Dhanasekar, K. R. Ishwarya, Dr.V.Balambica. (2021). IMPLEMENTING INDUSTRIAL ROBOTICS ARMS FOR MATERIAL HOLDING PROCESS IN INDUSTRIES. Harbin Gongye Daxue Xuebao/Journal of Harbin Institute of Technology, 53(9), 17–27. Retrieved from http://hebgydxxb.periodicales.com/index.php/JHIT/article/view/704.
41. Ahmed Ameer Arsalan Hadi , Karam Dheyaa Jirjees, G. B. L. I. H. S. (2021). AN ANALYSIS OF TOPOLOGY OPTIMIZATION ON ROBOT BY FINITE COMPONENT. Design

Engineering, 7336-7351. Retrieved from http://www.thedesignengineering.com/index.php/DE/article/view/3246. ISSN 0011-9342,

42. Dr.Qaysar Salih Mahdi, Mr.Ganesh Babu Loganathan, "Classification of Web Page by Using Neural Networks", Efflatounia, Volume: 5 Issue 2, Pages: 650 – 663, ISSN: 1110-8703.
43. Dr.Qaysar Salih Mahdi, Mr.Ganesh Babu Loganathan, "Modelling ofRadar Targets and Radar Cross Section For Air TrafficControl Radars", Efflatounia, Volume: 5 Issue 2, Pages: 664–674, ISSN: 1110-8703.
44. Babu Loganathan, Ganesh and M. Othman, Mohammad and Tahsin Yasin, Elham (2021) An Analysis on Garbage Removal Process by WSN thorugh Global System for Mobile Communication Media. REVISTA GEINTEC-GESTAO INOVACAO E TECNOLOGIAS, 11 (3). pp. 493-505. ISSN 2237-0722
45. BABU, L. G. (2021). MICROSTRUCTURE AND WEAR BEHAVIOUR OF A356-TIB2 NOVEL METAL MATRIX COMPOSITES. In Journal of the Balkan Tribological Association (Vol. 27, Issue 3, pp. 417–425). ISSN:1310-4772
46. Muthukumaran, S., Ganesan, M., Dhanasekar, J. and Loganathan, G.B. (2021). Path Planning Optimization for Agricultural Spraying Robots Using Hybrid Dragonfly – Cuckoo Search Algorithm. Alinteri Journal of Agriculture Sciences, 36(1): 412-419. -ISSN: 2587-2249. doi: 10.47059/alinteri/V36I1/AJAS21062.
47. Priyadharsini, S and Balaji Damodhar, T. S and Kannan, C and Babu Loganathan, Ganesh (2021) IMPROVED PERFORMANCE OF PHOTOVOLTAIC BASED EMBEDDED DUAL POWER SOURCE SL-QUASI Z SOURCE INVERTER FOR IM DRIVE. EPRA International Journal of Research and Development (IJRD), 6 (6). pp. 266-273.
48. P. Jeevitha, K. S. Elango, Ganesh Babu L, J. Ranjitha, S. Vijayalakshmi," Glycerol as a Key Reactant in the Production of 3-Hydroxypropanoic Acid using Engineered Microbes", AIP Conference Proceedings 2396, 030004 (2021). https://doi.org/10.1063/5.0066423
49. M. Othman, Mohammad and Ishwarya, K.R and Ganesan, Manikandan (2021) A Study on Data Analysis and Electronic Application for the Growth of Smart Farming. Alinteri Journal of Agriculture Sciences, 36 (1). pp. 209-218. ISSN 2564-7814
50. Sivama, S., Loganathanb, G., Harshavardhanaa, N., Kumarana, D., & Prasannaa, P. (2020). A comparative study of experimental and adaptive neuro fuzzy inference system based prediction model of machined AM60 magnesium alloy and its parameter effects. Materials Today: Proceedings, Volume 45, Part 2, 2021, Pages 1055-1062.
51. G.Sai Krishnan, K.Ilayaperumal, L.Ganesh Babu, S.Kumar, B.Sathish, R.Sanjana, "Investigation on the physical and mechanical characteristics of demostachya bipinnata reinforced with polyester composites" , Materials Today: Proceedings, Volume 45, Part 2, 2021, Pages 1134-1137.
52. G Shanmugasundar , M Vanitha , L Ganesh Babu , P Suresh , P Mathiyalagan , G Sai Krishnan and Mebratu Makos, "Fabrication and analysis of mechanical properties of PVC/Glass fiber/graphene nano composite pipes", Materials Research Express, ISSN: 2053-1591, Volume-7, Issue-11, May 2020, P.No 115303.
53. Babu, L.G. (2020). Influence on the tribological performance of the pure synthetic hydrated calcium silicate with cellulose fiber. In Journal of the Balkan Tribological Association, 26(4), 747–754.

54. Abdulghani Taha, Mohammed and Şah, Melike and Direkoğlu, Cem and Babu Loganathan, Ganesh (2020) Adaptive Wiener Filter And Non Linera Diffusion Based Deblurring And Denoising Images. Journal of critical reviews, 7 (3). pp. 908-915. ISSN 2394-5125
55. J. Aravind Kumar, D. Joshua Amarnath, A. Annam Renita and Ganesh Babu, "Activated Carbon Production From Biowaste Materials - Properties and Applications: A Review". Indian Journal of Environmental Protection, 40 (5). pp. 507-511.
56. P.Ramesh, G.Sai Krishnan, J.Pravin Kumar, M.Bakkiyaraj, Raghuram Pradhan, L.Ganesh babu, "A critical investigation on viscosity and tribological properties of molybdenum disulfide nano particles on diesel oil" , Materials Today: Proceedings, Volume 43, Part 2, 2021, Pages 1830-1833.
57. K. Rajendra Prasad, V. Manoj Kumar, G.Swaminathan, Ganesh Babu Loganathan, "Computational investigation and design optimization of a duct augmented wind turbine (DAWT)", Materials Today: Proceedings, Volume 22, Part 3, 2020, Pages 1186-1191.
58. Selvam, R., & Loganathan, G. B. (2019). Product detail and analysis of hydraulic quick releasing coupling. Materials Today: Proceedings, 22, 751–755. https://doi.org/10.1016/j.matpr.2019.10.081.
59. Suresh G., Ganesh B.L., Bharani K.S., Rajesh K.K. Influence of water absorption on glass fibre reinforced IPN composite pipes // Polímeros: Ciência e Tecnologia. 2019. Vol. 29 (3). P. 2019–2038.
60. Ganesh Babu L, Ramesh M and Ravichandran M 2019 Mechanical and tribological characteristics of ZrO2 reinforced Al2014 matrix composites produced via stir casting route Mater. Res. Express 4 115542115542.
61. Sivam Sundarlingam Paramasivam, S., Loganathan, G., Kumaran, D., Saravanan, K. et al., "Taguchi Based Vikor Method for Optimization of Cutting Parameters for Improving the Efficiency in Machining Process by Considering the Effect of Tool Nose Radius," SAE Technical Paper 2019-28-0138, 2019, https://doi.org/10.4271/2019-28-0138.
62. Loganathan, G., Saravanan, K., Rajendran, R., Sivam Sundarlingam Paramasivam, S. et al., "Investigation of Setting Input Process Parameters for Getting Better Product Quality in Machining of AM60 Magnesium Alloy - TOPSIS and ANOVA Approach," SAE Technical Paper 2019-28-0136, 2019, https://doi.org/10.4271/2019-28-0136.
63. Loganathan, G., Kumaran, D., Sivam Sundarlingam Paramasivam, S., Saravanan, K. et al., "Improvement of Mechanical Properties, and Optimization of Process Parameters of AISI 1050 Spheriodized Annealed Steel by Ranking Algorithm," SAE Technical Paper 2019-28-0143, 2019, https://doi.org/10.4271/2019-28-0143.
64. Sivam Sundarlingam Paramasivam, S., Kumaran, D., Loganathan, G., Saravanan, K. et al., "Development and Influence of Setting Process Variables in Single Point Incremental Sheet Metal Forming of AA 8011 Using Complex Proportional Assessment and ANOVA," SAE Technical Paper 2019-28-0064, 2019, https://doi.org/10.4271/2019-28-0064.
65. Thangaraj, M., Loganathan, G., Atif, A., and Palanisamy, S., "Multi Response Optimization on Machining Titanium Alloy Using Taguchi-DEAR Analysis in Abrasive Water Jet Cutting," SAE Technical Paper 2019-28-0070, 2019, https://doi.org/10.4271/2019-28-0070.
66. Loganathan, G., Sivam Sundarlingam Paramasivam, S., Kumaran, D., Saravanan, K. et al., "Experimental Study on Verification of Alloy ASTM A510 High-Speed Micro Turning by

Parameters Validation through Ranking Algorithm," SAE Technical Paper 2019-28-0071, 2019, https://doi.org/10.4271/2019-28-0071.

67. Sivam Sundarlingam Paramasivam, S., Loganathan, G., Saravanan, K., Kumaran, D. et al., "A Study on Mechanical Properties and Multi Response Optimization of Process Parameters for Showing Signs of Improvement Product Quality in Drilling $AlSi_7Cu_4$ Utilizing GRA in Taguchi Method," SAE Technical Paper 2019-28-0058, 2019, https://doi.org/10.4271/2019-28-0058.
68. Sivam Sundarlingam Paramasivam, S., Loganathan, G., Saravanan, K., Kumaran, D. et al., "Optimization of Machining Process Parameters for Minimizing the Waste Stream Response through Multi-Objective Optimization," SAE Technical Paper 2019-28-0062, 2019, https://doi.org/10.4271/2019-28-0062.
69. S.P.S.S.Sivam G.B. Loganathan and L. Ganesh Babu and D. Kumaran. 2019. Enhancing the Mechanical Properties and Formability of Cold Rolled Closed Annealed Sheet for Automobile Applications Int J. Vehicle Structures & Systems. 11 15-20.
70. Muralikrishna, M.V.V.; Surya Kumari, T.S.A.; Gopi, R.; Loganathan, G.B. Development of mechanical properties in banana fiber composite. Mater. Today Proc. 2020, 22, 541–545.
71. S.P. Sundar Singh Sivam et al.2019 Analysis of Product Quality through Mechanical Properties and Determining Optimal Process Parameters of Untreated and Heat Treated ALSI 1050 Alloy during Turning Operation Mater. Sci. Forum. 969 876-881.
72. L. Ganesh Babu, G. Sai Krishnan & N. Siva Shanmugam, "Microstructural and Corrosion Studies by Immersion IN 3.5wt % NaCl Environment on Mg-6Al-1Zn-XCa ALLOY with Ca Addition and Aged at Different Temperatures", International Journal of Mechanical and Production Engineering Research and Development (IJMPERD) Vol. 9, Issue 3, Jun 2019, 1553-1562, ISSN (P): 2249-6890; ISSN (E): 2249-8001.
73. G. Sai Krishnan , L. Ganesh Babu & N. Siva Shanmugam "Experimental investigation of wear behaviour of A356-Tib2 metal matrix composites", International Journal Of Mechanical And Production Engineering Research And Development (IJMPERD) Vol. 9, Issue 3, Jun 2019, 1353-1362. ISSN (P): 2249-6890; ISSN (E): 2249-8001.
74. Abubakr, M., & Kaya, T. (2021). A Comparison of E-Government Systems Between Developed and Developing Countries: Selective Insights From Iraq and Finland. International Journal of Electronic Government Research (IJEGR), 17(1), 1-14. http://doi.org/10.4018/IJEGR.2021010101
75. Sai Krishnan G and Loganathan G B 2019 Development of superhydrophobic nanocomposite coatings on FRP sheet surface for antiicing and wear-resistance applications(August 5, 2019) Proc. of Int. Conf. on Recent Trends in Computing, Communication & Networking Technologies (ICRTCCNT).
76. Ganesh Babu Loganathan, S. Kalyan Kumar, S.P. Sundar Singh Sivam, K. Saravanan, S. RajendraKumar, "Experimental Investigation and Optimization of Wire Cut EDM Parameters for Performance Measures of Heat Treated SS304: Ranking Algorithm and Anova Approach" International Journal of Recent Technology and Engineering (IJRTE) Volume-7, Issue-6, March 2019, ISSN: 2277-3878.
77. S Dhanraj et al 2019, "An Efficiency Study On Water Extraction From Air Using Thermophoresis Method" IOP Conf. Ser.: Mater. Sci. Eng. 574 012003.

78. Arivazhagan, R.; Prakash, A. S.; Kumaran, P.; Sankar, S.; Loganathan, B. G.; Arivarasan, A., 2020. "Performance analysis of concrete block integrated with PCM for thermal management", Materials Today: Proceedings 22, 370 – 374.
79. S.P. Sundar Singh Sivam, Ganesh Babu Loganathan, P.R. Shobana Swarna Ratna, G. Balakumaran , "Improvement of Product Quality by Process Parameter Optimization of AISI 1050 by Different Heat Treatment Conditions: Ranking Algorithm and ANOVA", International Journal of Innovative Technology and Exploring Engineering (IJITEE) Volume-8 Issue-5 March, 2019, PP.30-35, ISSN: 2278-3075.
80. S. Ashok Kumar, Ganesh Babu Loganathan, P.R. Shobana Swarna Ratna, G. Balakumaran, S.P. Sundar Singh Sivam, "Determination of Taguchi Grey Relation Analysis to Influence the Tool Geometry and Cutting Parameters of the Ti-6Al-4V Alloy to Achieve Better Product Quality" , International Journal of Innovative Technology and Exploring Engineering (IJITEE) Volume-8 Issue-5 March, 2019, PP.212-217, ISSN: 2278-3075.
81. S.P. Sundar Singh Sivam, Ganesh Babu Loganathan, K. Saravanan, S. RajendraKumar, "Multi-Response Enhancement of Drilling Process Parameters for AM 60 Magnesium Alloy as per the Quality Characteristics utilizing Taguchi-Ranking Algorithm and ANOVA", International Journal of Innovative Technology and Exploring Engineering (IJITEE) Volume-8 Issue-4, February 2019, PP.437-440, ISSN: 2278-3075.
82. Ganesh Babu Loganathan, "An Identical Machine-Adaptive Algorithm Based Blockchain Process and Predicting Secret Data From Hacking In Computer Numerical Control Applications", International Journal of Mechanical and Production Engineering Research and Development (IJMPERD) Vol. 9, Special Issue 1, Jan 2019, PP.510-522, ISSN(P): 2249-6890; ISSN(E): 2249-8001.
83. S.P. Sundar Singh Sivam, Ganesh BabuLoganathan, K. Saravanan, S. RajendraKumar, "Outcome of the Coating Thickness on the Tool Act and Process Parameters When Dry Turning Ti–6Al–4V Alloy: GRA Taguchi & ANOVA", International Journal of Innovative Technology and Exploring Engineering (IJITEE) ISSN: 2278-3075, Volume-8, Issue-4, February 2019 PP. 419-423.
84. S. M. Pirrung, L. A. M. van der Wielen, R. F. W. C. van Beckhoven, E. J. A. X. van de Sandt, M. H. M. Eppink, and M. Ottens, "Optimization of biopharmaceutical downstream processes supported by mechanistic models and artificial neural networks," Biotechnol. Prog., vol. 33, no. 3, pp. 696–707, 2017.